

Projectile-charge dependence of quasi-free-electron bremsstrahlung

著者	石井 慶造
journal or publication title	Physical review. A
volume	27
number	4
page range	2225-2228
year	1983
URL	http://hdl.handle.net/10097/35222

doi: 10.1103/PhysRevA.27.2225

Projectile-charge dependence of quasi-free-electron bremsstrahlung

K. Ishii and K. Sera

Cyclotron and Radioisotope Center, Tohoku University, 980 Sendai, Japan

H. Arai

Department of Physics, Faculty of Science, Tohoku University, 980 Sendai, Japan

S. Morita and K. Tokuda

Research Center of Ion Beam Technology, Hosei University, Kajinocho, Koganei, 184 Tokyo, Japan

(Received 29 November 1982)

Continuum x rays induced by bombardments of a Be target with 20.14-MeV/amu protons and ³He²⁺ ions have been measured with a Si(Li) detector in the direction of 90° with respect to the incident beam. Differences in the x-ray-production cross sections multiplied by the x-ray energy $\hbar\omega$ [$\hbar\omega [\sigma_h(\hbar\omega)/4 - \sigma_p(\hbar\omega)]$] and ratio of the cross sections $R(\hbar\omega) [\equiv \sigma_h(\hbar\omega)/4\sigma_p(\hbar\omega)]$ for the proton and ³He²⁺-ion impact, where $\sigma_h(\hbar\omega)$ and $\sigma_p(\hbar\omega)$ are the x-ray-production cross sections for proton and ³He²⁺-ion impact, respectively, were obtained as a function of the x-ray energy. Both the difference and the ratio show peaks in the region where the x-ray energy is equal to the relative kinetic energy between the projectile and the inner-shell electron to be scattered by the projectile. From the comparison with a theory of quasi-free-electron bremsstrahlung based on the impulse approximation, it is found that this peak corresponds to the maximum of the velocity-distribution function of the inner-shell electron. Furthermore, the contribution of the radiative electron-capture process in the case of proton and ³He²⁺ impact is clearly found.

Recently,¹ we have bombarded targets of Be, C, and Al with 6–40-MeV protons and have found a new component of continuum x rays. These continuum x rays are predominant in the region where the x-ray energy $\hbar\omega$ is smaller than the energy $T_r \equiv \frac{1}{2}m_e V_p^2$, where m_e is the electron mass and V_p is the projectile velocity, and the Doppler effect is definitely observed in the angular distributions of these x rays.² From these experimental results, the x rays have been well understood in terms of the bremsstrahlung produced by the orbital electrons scattered by the projectile Coulomb field; we call this process the quasi-free-electron bremsstrahlung (QFEB). The

projectile-energy dependence and the angular dependence of QFEB have been well explained by a simple theory assuming that the orbital electrons are free. Further, a calculation taking into account the velocity distribution of orbital electrons has been developed,² and it was found that the spectrum of QFEB in the vicinity of the high-energy limit of $\hbar\omega = T_r$ is sensitively dependent on the velocity distribution of orbital electrons.

On the basis of the impulse approximation which Jakubassa and Kleber have developed for the bremsstrahlung in heavy-ion reaction,³ a more accurate formula for the cross section of QFEB can be given by

$$\sigma^{QFEB} = \sum_i n_i \int_{-\infty}^{v_i^{\max}} \rho_i(v_z) dv_z \frac{\hbar\omega}{\hbar\omega'} \left(\frac{T_r'}{T_r} \right)^{1/2} \sigma^{\text{brems}}(T_r', \hbar\omega', \theta) \tag{1}$$

with

$$v_i^{\max} = \frac{1}{2} V_p [1 - (\hbar\omega + I_i)/T_r] ,$$

$$\hbar\omega' = \hbar\omega + I_i + \frac{1}{2} m_e v_z^2 ,$$

$$T_r' = T_r (1 - v_z/V_p)^2 .$$

In Eq. (1), n_i represents the number of electrons in the i shell, $\rho_i(v_z)$ is the integrated velocity distribution of the i -shell electrons and has been defined by Eq. (8) in Ref. 2, I_i is the ionization energy for the

i -shell electrons, and $\sigma^{\text{brems}}(T_r', \hbar\omega', \theta)$ is the differential cross section of the bremsstrahlung production for free electrons which have the energy T_r' in the initial state and emit photons of the energy $\hbar\omega'$ in the direction of θ and has been shown by Eq. (1) in Ref. 2. Equation (1) agrees with our previous formula of Eq. (9) in Ref. 2 in the case of neglecting the potential energy of the orbital electron.

In accordance with the electron bremsstrahlung accompanied by the Coulomb deflection discussed in the previous paper,² the production cross section of

the bremsstrahlung in the laboratory system can be approximated, in the direction of 90° for the x-ray emission, by

$$\sigma^{\text{brems}}(T_r', \hbar\omega', 90^\circ) \approx \begin{cases} \frac{Z_p^2}{\pi} r_0^2 \alpha \frac{m_e C^2}{\hbar\omega'} \frac{1}{T_r'} \left[\left(\frac{3}{4} - \frac{T}{4} \right) \ln \frac{1+\sqrt{T}}{1-\sqrt{T}} + \frac{1}{2} \sqrt{T} \right], & \text{for } T > \delta T \\ \frac{Z_p^2}{\pi} r_0^2 \alpha \frac{m_e C^2}{\hbar\omega'} \frac{1}{T_r'} \frac{1}{\sqrt{T_r'}} 4\pi Z_p \sqrt{R_y}, & \text{for } 0 \leq T \leq \delta T, \end{cases} \quad (2)$$

with

$$T = (T_r' - \hbar\omega')/T_r',$$

where the notations r_0 , α , $m_e C^2$, and R_y have been explained in Ref. 2, Z_p is the atomic number of the projectile which is now a target nucleus for the elec-

tron bremsstrahlung in the case of QFEB, and the value of δT is small enough to realize the above approximation. When the velocity of orbital electrons is small in comparison with that of the projectile, as in the present case, the differential cross section of QFEB is given from Eqs. (1) and (2) by

$$\sigma^{\text{QFEB}}(Z_p, V_p, 90^\circ, \hbar\omega) = \frac{Z_p^2}{\pi} r_0^2 \alpha \frac{m_e C^2}{\hbar\omega} \left\{ \sum_i n_i \int_{-\infty}^{v_i^{\text{max}}} \left(\frac{\hbar\omega}{\hbar\omega'} \right)^2 \left[\left(\frac{3}{4} - \frac{T}{4} \right) \ln \left(\frac{1+\sqrt{T}}{1-\sqrt{T}} \right) + \frac{1}{2} \sqrt{T} \right] \frac{\rho_i(v_z)}{(T_r'/T_r)^{1/2}} dv_z \right. \\ \left. + Z_p \frac{4\pi\alpha c}{\hbar\omega} \delta T \sum_i n_i \frac{T_r}{T_r + \hbar\omega + I_i} \left(\frac{\hbar\omega}{\hbar\omega + I_i + \frac{1}{2} m_e (v_i^{\text{max}})^2} \right)^3 \rho_i(v_i^{\text{max}}) \right\}. \quad (3)$$

The second term of Eq. (3) directly reflects the velocity distribution and is proportional to the third power of the projectile charge Z_p in contrast to the Z_p^2 dependence of the first term. It is therefore expected that the velocity distribution of orbital electrons would give rise to a difference in the QFEB cross sections between two kinds of projectiles of equivelocity with the atomic charge z_1 and z_2

$$\hbar\omega \times [\sigma^{\text{QFEB}}(z_2, V_p, 90^\circ, \hbar\omega)/z_2^2 \\ - \sigma^{\text{QFEB}}(z_1, V_p, 90^\circ, \hbar\omega)/z_1^2]$$

and also effects the ratio between the continuum x-ray-production cross section

$$R(\hbar\omega) \equiv \frac{z_1^2 \sigma(z_2, V_p, \hbar\omega)}{z_2^2 \sigma(z_1, V_p, \hbar\omega)}.$$

Beams of 20.21-MeV/amu protons and 20.23-MeV/amu $^3\text{He}^{2+}$ ions from the AVF cyclotron of Tohoku University bombarded a Be target of 4.67-mg/cm² thickness, which was set at 45° with respect to the beam. By taking into account the energy spread in the target, the beam energies were estimated to be 20.14 ± 0.07 MeV/amu for protons and 20.14 ± 0.09 MeV/amu for $^3\text{He}^{2+}$ ions, so that the mean projectile energy in the target is in good agreement for both kinds of projectile. The x rays have been measured with an ORTEC Si(Li) detector in the direction 90° to the beam. Continuum background radiation induced by the Compton scattering of γ rays from nuclear reactions in the Si(Li) detector has been measured by putting a 2-mm copper absorber in front of the detector. Differential cross sections for

the continuum x-ray production obtained after subtracting the background are shown in Fig. 1 as a function of the x-ray energy $\hbar\omega$. In this figure, the dashed and the solid lines stand for proton and $^3\text{He}^{2+}$ bombardments, respectively. The ordinate shows the cross section multiplied by the x-ray energy and divided by a square of the projectile charge

$$[d\sigma^{\text{brems}}/d\Omega d(\hbar\omega)]\hbar\omega/Z_p^2.$$

Peaks appearing in the low-energy region are for K x rays of impurity elements Cr, Fe, Ni, and Ca contained in the Be target. The main part of the continuum x rays in the region of $\hbar\omega \leq T_r$ is due to the QFEB process, while the secondary electron bremsstrahlung (SEB) is predominant in the region of $\hbar\omega \geq T_r$. In the vicinity of $\hbar\omega = T_r'$ a difference is seen between the spectra for proton and for $^3\text{He}^{2+}$ impact, whereas the spectra are in good agreement in the other region. In order to interpret this difference in the cross sections, the contributions of Z_p^3 dependence of QFEB and also the radiative electron capture (REC), which is predominant in the region of $\hbar\omega \approx T_r - I_i$, are to be considered. Figure 2 shows the difference between the cross sections for $^3\text{He}^{2+}$ -ion and proton impact

$$\hbar\omega \times [\frac{1}{4} \sigma_h(\hbar\omega) - \sigma_p(\hbar\omega)]$$

obtained from the experiment and from the theoretical calculations of QFEB and REC.⁴ It is found in this figure that the experimental value makes a peak at $\hbar\omega \approx T_r$. Peaks in the region of $\hbar\omega \approx 7$ KeV are due to the K x rays from the impurity elements. The dotted line and the dashed line in Fig. 2 show the

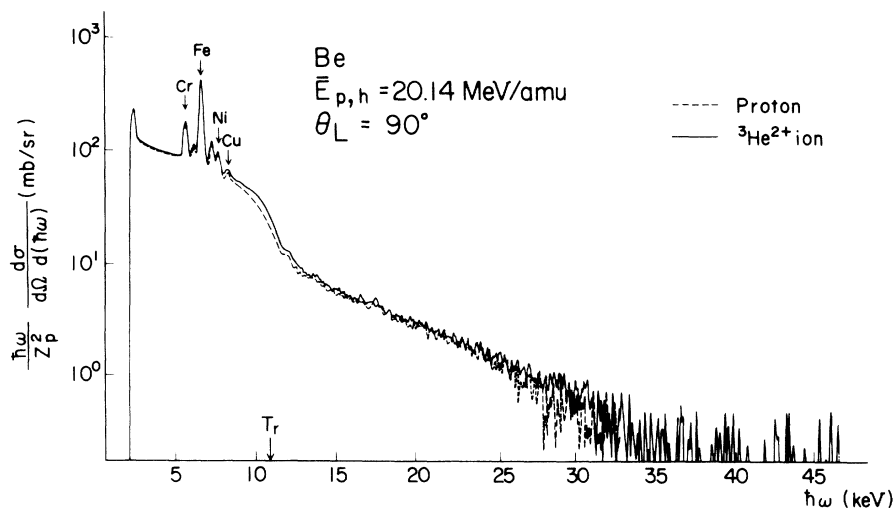


FIG. 1. X-ray spectra for the Be target bombarded with 20.11-MeV/amu protons (dashed line) and 20.33-MeV/amu $^3\text{He}^{2+}$ ions (solid line), measured in the direction 90° with respect to the incident beam. The ordinate shows the differential cross sections multiplied by the x-ray energy and divided by the square of the projectile charge.

difference

$$\hbar\omega \times [\sigma_h^{\text{QFEB}}(\hbar\omega)/4 - \sigma_p^{\text{QFEB}}(\hbar\omega)]$$

calculated from Eq. (1), respectively, for the 1s electrons of the Be target and for the 2s electrons, and the dot-dashed line is the difference in cross section for REC between the two kinds of projectile

$$\hbar\omega \times [\sigma_h^{\text{REC}}(\hbar\omega)/4 - \sigma_p^{\text{REC}}(\hbar\omega)]$$

calculated in terms of the impulse approximation developed by Kleber and Jakubassa.⁴ The solid line shows the sum of these differences in the cross sections for QFEB and REC. It is seen that the calculations based on the impulse approximation for QFEB and REC can quite well explain the present experimental results. Furthermore, the agreement between experiment and theory is also found in the ratio of continuum x-ray-production cross sections $R(\hbar\omega)$.

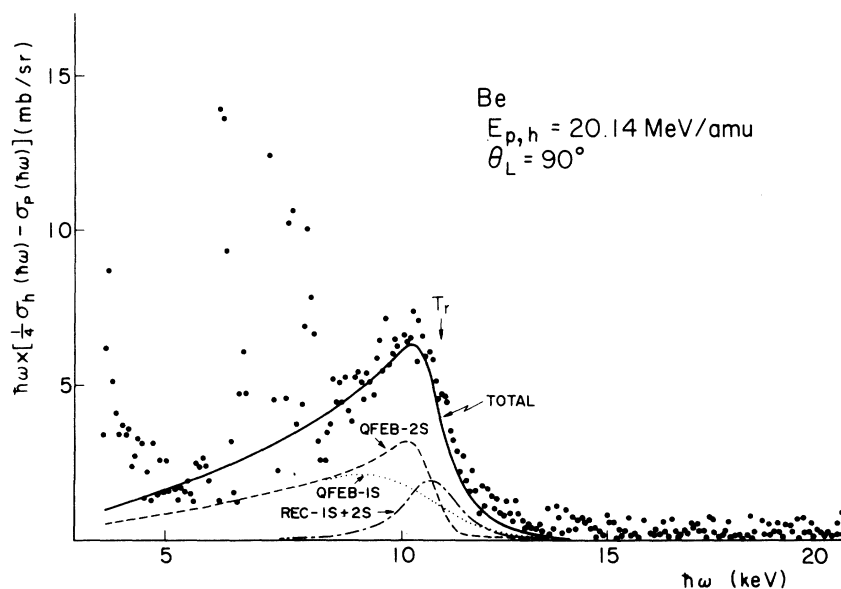


FIG. 2. Difference in cross sections for $^3\text{He}^{2+}$ -ion and proton impact $\hbar\omega [\sigma_h(\hbar\omega)/4 - \sigma_p(\hbar\omega)]$. The dotted line is the theoretical value for QFEB calculated for the 1s electron of the Be target estimated from Eq. (1) and the dashed line is for the 2s electrons. The dot-dashed line is the difference in cross sections for the REC process calculated from the formula of Kleber and Jakubassa (Ref. 4). The solid line is the sum of the differences calculated for QFEB and REC.

Figure 3 shows the ratio $R(\hbar\omega)$ obtained from experiment and from the theoretical calculations of QFEB, SEB,² and REC.⁴ As seen in Fig. 3, $R(\hbar\omega)$ peaks again at $\hbar\omega \approx T_r$. Fluctuation of $R(\hbar\omega)$ appearing in the region of $\hbar\omega \approx 7$ keV is due to the K x rays from the impurity elements. In this figure, the dashed line and the solid line show the theoretical calculations of $R(\hbar\omega)$, respectively, of QFEB plus SEB and of QFEB plus SEB plus REC which are expressed by

$$R(\hbar\omega) = \frac{\sigma_h^{\text{QFEB}}(\hbar\omega) + \sigma_h^{\text{SEB}}(\hbar\omega)}{4[\sigma_p^{\text{QFEB}}(\hbar\omega) + \sigma_p^{\text{SEB}}(\hbar\omega)]} \quad (4)$$

and

$$R(\hbar\omega) = \frac{\sigma_h^{\text{QFEB}}(\hbar\omega) + \sigma_h^{\text{SEB}}(\hbar\omega) + \sigma_h^{\text{REC}}(\hbar\omega)}{4[\sigma_p^{\text{QFEB}}(\hbar\omega) + \sigma_p^{\text{SEB}}(\hbar\omega) + \sigma_p^{\text{REC}}(\hbar\omega)]}, \quad (5)$$

where $\sigma^{\text{SEB}}(\hbar\omega)$ is evaluated using the expression for the cross section of SEB previously developed² for the case of $V_p \gg v_e$, where v_e is the velocity of orbital electrons in the target. In Fig. 3, the contribution of the REC process seems to be more pronounced than in the case of the difference of the cross sections.

It is thus concluded that, as has been observed in the x-ray spectrum of REC,⁵ the velocity distribution of the orbital electron has a large effect on both the difference and the ratio of the cross sections for QFEB between proton and ${}^3\text{He}^{2+}$ -ion impact and also

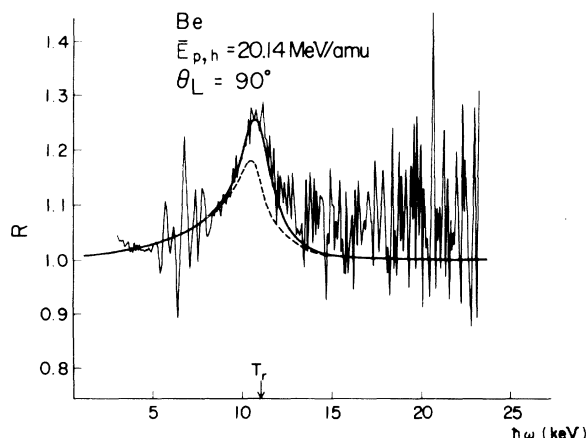


FIG. 3. Ratio of cross sections for proton impact to those for ${}^3\text{He}^{2+}$ -ion impact $R(\hbar\omega) \equiv \sigma_h(\hbar\omega)/4\sigma_p(\hbar\omega)$. The dashed line is estimated from Eq. (4) in the text using the theories of QFEB and SEB developed in Ref. 2. The solid line is calculated by taking the REC process into consideration.

that the contribution of REC is clearly found even for proton and ${}^3\text{He}^{2+}$ -ion impact, though the REC process has been well studied in the case of heavy-ion impact.

The authors wish to express their thanks to Dr. H. Tawara and Dr. A. Yamadera for their cooperation in data acquisition and for useful discussions.

¹A. Yamadera, K. Ishii, K. Sera, M. Sebata, and S. Morita, Phys. Rev. A **23**, 24 (1981).

²T. C. Chu, K. Ishii, A. Yamadera, M. Sebata, and S. Morita, Phys. Rev. A **24**, 1720 (1981).

³H. Jakubassa and M. Kleber, Z. Phys. A **273**, 29 (1975).

⁴M. Kleber and H. Jakubassa, Nucl. Phys. **A252**, 152 (1975).

⁵E. Spindler, H.-D. Betz, and F. Bell, J. Phys. B **10**, L561 (1977).